Available online at www.sciencedirect.com
ScienceDirect
Journal of Power Sources 171 (2007) 381–387
JOURNAL OF POWER SOURCES
www.elsevier.com/locate/jpowsour

$Ru_xCr_ySe_z$ electrocatalyst loading and stability effects on the electrochemical performance in a PEMFC

K. Suárez-Alcántara [a], A. Rodríguez-Castellanos [a], S. Durón-Torres [b], O. Solorza-Feria [a,*]

[a] *Depto. Química, Centro de Investigación y de Estudios Avanzados del IPN, A. Postal 14-740, 07360 México D.F., Mexico*
[b] *Unidad A. Ciencias Químicas, Universidad Autónoma de Zacatecas, Km. 0.5 Carretera a Cd. Cuauhtémoc, Guadalupe, 98600 Zacatecas, Mexico*

Received 23 April 2007; received in revised form 31 May 2007; accepted 4 June 2007
Available online 30 June 2007

Abstract

The present paper presents a study of the $Ru_xCr_ySe_z$ chalcogenide electrocatalyst based on physical–chemical characterization through scanning electron (SEM), atomic force (AFM) microscopy and energy dispersion elemental analysis (EDS), thermal stability using differential scanning calorimeter (DSC), electrochemical kinetics towards the oxygen reduction reaction (ORR) in acid media by rotating ring-disk electrode (RRDE) and single and three-stack membrane-electrode assembly (MEA) performance as a function of catalyst loading (10%, 20% and 40% W from 0.2 to 2 mg cm^{-2}). Results indicate an electrocatalyst with chemical composition of $Ru_6Cr_4Se_5$. AFM images showed 80–160 nm nanoparticle agglomerates. Good thermal stability of the cathode $Ru_6Cr_4Se_5$ was established after 100 h of continuous operation. The electrochemical kinetics study (RRDE) resulted in a electrocatalyst with high activity towards the ORR, preferentially proceeding via $4e^-$ charge transfer pathway towards water formation (*i.e.*, $O_2+4H^++4e^-\rightarrow 2H_2O$), with a maximum of 2.8% H_2O_2 formation at 25 °C. Finally, MEA tests revealed a maximum power density of 220 mW cm^{-2} with a catalyst loading of 20 wt% at 1.6 mg cm^{-2}.

Keywords: Ruthenium-based electrocatalyst; ORR; PEMFC electrocatalyst loading

1. Introduction

Polymer electrolyte membrane fuel cell (PEMFC) is becoming an interesting power source for many applications varying from small size portable units to large stationary systems. One of the actual challenges of the PEMFC technology resides in the loading reduction of the expensive Pt electrocatalyst and/or its replacement with a less expensive material with comparable activity [1]. Several metallic and bimetallic selective electrocatalysts in the form of nanoclusters have been investigated for the cathodic reaction in PEMFCs. The oxygen reduction reaction (ORR) has been the focus of extensive research aimed to find novel materials with high activity and stability in extended operation regimes. Recent studies also are being focused to reduce the high overpotential present during this reaction to overcome the inherent cathode slow kinetics. The techniques used in the preparation of these novel electrocatalysts included micro dispersion [2], colloidal adsorption [3], ion-exchange and chemical routes [4,5]. Transition-metal carbonyl compounds have been extensively studied in our group through organo-metallic chemistry due to their good balance between reactivity and stability. Previous communications has shown that the decarbonylation of transition-metal cluster compounds in organic solvent produced highly dispersed and supported-cluster catalyst on different substrates. The reaction of these clusters with an elemental chalcogenide generates a variety of mono- and polynuclear compounds with coordination center of *d*-states [6–8]. It has been reported that ruthenium-based electrocatalyst presents reasonable stability and good activity towards the ORR in acid medium [9–12]. The interest in ruthenium as chalcogenide electrode bearing chromium atoms has leaded this research group to investigate the feasibility of using this material as cathode in fuel cells. The rationale for incorporating chromium into ruthenium selenide is to improve the stability of the new compound as well as to enhance the electrocatalytic activity through the synergistic effects of the two metals included in this chalcogenide electrocatalyst ($Ru_xCr_ySe_z$). The synthesis methodology, physicochemical and electrochemical

* Corresponding author. Tel.: +52 55 5061 3715; fax: +52 55 5061 3389.
E-mail address: osolorza@cinvestav.mx (O. Solorza-Feria).

0378-7753/$ – see front matter © 2007 Elsevier B.V. All rights reserved.
doi:10.1016/j.jpowsour.2007.06.201

characterization of $Ru_xCr_ySe_z$ catalyst was reported previously [8]. In this work the study of the kinetics pathway, the amount of hydrogen peroxide production in the ORR on $Ru_xCr_ySe_z$ catalyst (thin-film rotating ring-disk electrode) and a comparative behavior with respect to 10 wt% Pt/C (E-TEK) disk is reported. After electrochemical analysis, the study of the electrocatalyst as cathode was performed. In addition of its optimum performance in a membrane–electrode assembly (MEA) of a single polymer electrolyte fuel cell, research presents the performance of a three home-made MEAs fuel cell stack. The performance achieved at different temperatures and catalyst loadings suggests that $Ru_xCr_ySe_z$ electrocatalyst could be considered to be a suitable candidate to be used as cathode in H_2/O_2 – air PEMFC.

2. Experimental

2.1. Physical characterization

Elemental analysis was obtained with an EDS connected to an electronic scanning microscope SEM, FEI Sirion XL30 operated at 20 kV. Atomic force microscopy images were obtained in a JEOL scanning probe microscope JSPM-4210 in tapping mode, with a resonant frequency at 150 kHz and an Ultra-Sharp silicon cantilever NSC 12 was used to analyze the topography and profiles of the electrocatalyst samples. Finally, a Perkin Elmer DCS7 differential scanning calorimeter was used to obtain thermograms between 30 and 200 °C at 5.0 °C min^{-1} scanning speed. The calorimeter was calibrated with metallic Zn and operated by Pyris Software.

2.2. Electrochemical characterization

RRDE experiments were performed in a Pine AFCBP1 bipotentiostat. The working electrode employed in all samples was a commercial MT28 Pine glassy carbon disk (diam = 4.57 mm), covered with a thin-film catalytic suspension (ink) and Au ring with 4.93 mm inner and 5.38 mm outer diameters, with 0.22 of nominal collection efficiency. The $Ru_xCr_ySe_z$ catalyst was synthesized in 1,6-hexanediol at 220 °C for 2 h, as previously reported [8]. The catalytic ink or suspension was prepared with 1 mg of $Ru_xCr_ySe_z$ catalyst, 14 μL of 5 wt% Nafion® (Du Pont, 1100 EW), 100 μL water and 96 μL ethyl alcohol (spectrum grade). Six microlitters of this ink containing ~0.17 mg/cm^2 of catalyst, was deposited onto the glassy carbon electrode surface (geometric area = 0.164 cm^2) and dried at room temperature. The reference electrode used was an Hg/Hg_2SO_4/0.5 M H_2SO_4 (MSE = 0.68 V/NHE) and a Pt mesh as a counter electrode. The potentials in the electrochemical experiments were referred to NHE. The electrolyte was a 0.5 M H_2SO_4 solution prepared from double-distilled water which was degassed with nitrogen for the working electrode activation and saturated with oxygen for 10 min before each ORR electrochemical measurement. The rotation speed of the working electrode was varied between 200 and 2500 rpm, maintaining a scan rate of 5 mV s^{-1}. The ring potential was kept at +1.40 V (NHE) during all the electrochemical experiments. The collection efficiency, N, was obtained experimentally from the slope of an i_R versus i_D plot at different rotation speeds using as electrolyte a 5×10^{-3} M $K_3Fe(CN)_6$ solution in 0.1 M K_2SO_4. A value of $N = 0.13$ was found for this arrangement.

2.3. Membrane–electrode assembly (MEA) preparation and characterization

Membrane electrode assemblies were prepared using Nafion® 112 membranes. An anodic loading of 0.8 mg cm^{-2} of 10 wt% Pt/C (E-TEK) was used in all MEAs prepared. Cathode catalyst loading was varied between 0.2 and 2.0 mg cm^{-2} at 10, 20 and 40 wt% of $Ru_xCr_ySe_z$ dispersed carbon Vulcan XC-72. The catalytic suspension was prepared by mixing 50 μL of Nafion® 5 wt% (Du Pont, 1100 EW) and 1.5 mL of ethyl alcohol per each 3.6 mg of carbon Vulcan XC.72. The gas diffusion medium at cathode and anode sides were Teflon treated carbon papers (ElectroChem). The catalytic suspension was sprayed onto a Nafion® 112 membrane using a lab-made electronic automatic device. The membrane was previously treated with H_2O_2 and H_2SO_4 as reported in literature [8]. In order to prevent ohmic resistance and to form good contact between the electrodes and the polymer membrane, the MEAs were hot pressed at 120 °C and 4.4 kg cm^{-2} for 1.5 min, resulting in a active area of the anode and cathode of 5 cm^2. PEMFC performance experiments were carried out in an Electrochem Fuel Cell Test System 890B. High purity H_2 and O_2 were fed to the single fuel cell at 50 cc min^{-1}. The fuel cell performance was measured between 40 and 80 °C at 30 psi for both gases. The fuel cell station was equipped with a humidifying system for the reactant gases; humidifier temperatures were fixed at 5 °C higher than cell temperature.

2.4. Fuel cell stack fabrication

A small fuel cell stack was designed and fabricated using Nafion® 112 polymer membranes. Three MEAs of 9.61 cm^2 geometric surface area per side were prepared by using carbon cloths as gas diffusion medium and 10 wt% Pt/C (E-TEK) as anodes with a catalyst loading of 0.5 mg cm^{-2}. The catalyst loading of 20 wt% $Ru_xCr_ySe_z$ dispersed on Vulcan on the cathode sides was 1.6 mg cm^{-2}. The catalytic ink was prepared as described above and it was sprayed over a membrane by means of a lab-made electronic automatic device. The gas diffusion medium at cathode side was Teflon treated carbon paper (ElectroChem). The MEA was hot pressed at 120 °C and 4.4 kg/cm^2 between two metallic heating plates without the anode carbon cloth. The carbon cloths were then fixed only by pressing the bipolar plates during the stack construction. Gaskets and seals of the stack were home-molded with high temperature resistant silicone. Bipolar plates were home-machined and made of high-density graphite (POCO) and end plates were aluminum-machined. All stack elements were home designed. Stack PEMFC performance was carried out in an Electrochem Fuel Cell Test System 890B. The performance was measured at

80 °C and 10 psi pressure for both gases. High purity humidified H_2 and O_2 (50 cc min^{-1}) were fed to the stack.

3. Results and discussion

3.1. Physical characterization

Fig. 1 shows a DCS curve obtained from the thermal response in the 30–200 °C range of the as synthesized powder catalyst. There is an exothermic peak at 125.5 °C probably due to a rearrangement reaction within the catalyst clusters. Despite this peak, it was found that the electrocatalyst presents a good thermal stability above the operation limits when it is used as cathode in a PEMFC operational range. From EDS results, the estimated elemental analysis gave an atomic composition of the catalyst as $Ru_6Cr_4Se_5$. However, because the synthesis method is not selective, it cannot be concluded that this corresponds to a real composition. AFM was used to obtain the surface morphology which images are shown in Fig. 2. Results suggest that the catalyst is composed of nanoparticles agglomerates in the range of 80–160 nm size. The surface appears to be a highly rough a fractal-like type. The catalyst morphology of the surface at 2 μm (Fig. 2a) is highly rough and it is also maintained at approximately 100 nm (Fig. 2b). It can be considered that the particle size is somewhat huge compared with typical particle sizes (5–10 nm) synthesized by this method, and can be attributed to the sintering process which could play an important role in the stability of the catalyst during long periods of time.

3.2. Electrochemical characterization

In a previous work [8] we have shown that $Ru_xCr_ySe_z$ films deposited on glassy carbon electrodes efficiently catalyzed the reduction of oxygen in acid medium. In this study RRDE technique is used to study the kinetics of the molecular oxygen

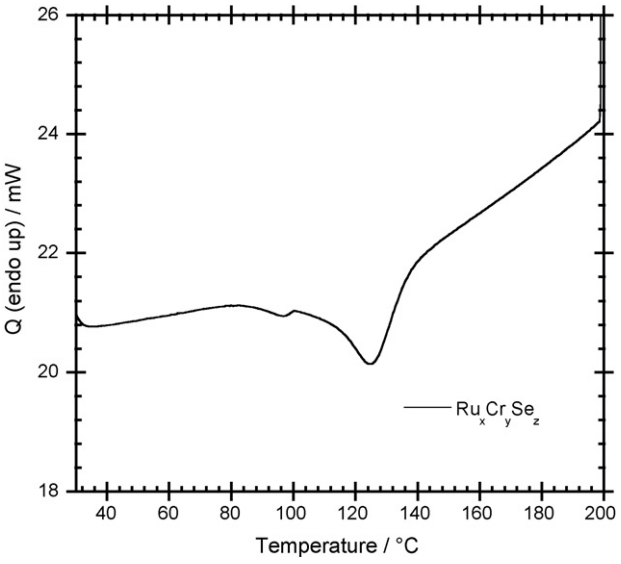

Fig. 1. Differential scanning calorimetry curves of $Ru_xCr_ySe_z$ catalyst.

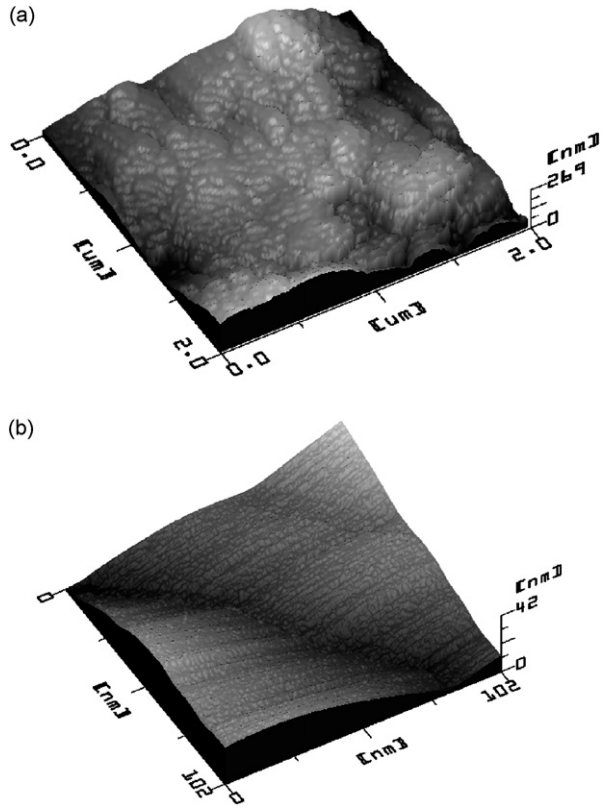

Fig. 2. AFM surface morphology of $Ru_xCr_ySe_z$ as-synthesized in 1,6-hexanediol at 220 °C. (a) Cluster catalyst at 2 μm and (b) cluster catalyst at 100 nm.

reduction reaction in order to determine the amount of hydrogen peroxide produced and the pathway of the electrochemical reaction. Steady state polarization curves obtained for the ORR in the disk electrode and the currents for the hydrogen peroxide oxidation in the ring are shown in Fig. 3. In the out-gassed solution with N_2 only a small residual nonfaradaic current is observed in the disk electrode, while in the O_2 saturated solution an increase in the diffusion current in the disk is observed as a function of rotation speed. The disk currents did not reach a perfect plateau of the diffusion limited currents, and this is due to the small amount of catalyst (0.17 mg/cm^2) on the thin film formed on the glassy carbon electrode with the catalytic ink, but it is clearly defined its dependency with the rotating speed. The ring currents reached a maximum value near 0.25 V (NHE), similar to the electrochemical behavior of some ruthenium-based catalysts reported previously [5,13]. A comparison of the electrochemical response with a 10 wt% Pt/C disk at 1600 rpm is depicted in the same Fig 3. In this Figure, a shift of 0.1 V of the open circuit potential towards more cathodic values and an increase of the current disk in all the wide range of the potential is observed. Also a small amount of hydrogen peroxide on the ring electrode is detected. Fig. 4 presents the average percentage of hydrogen peroxide formed as a by-product of the oxygen reduction reaction on the $Ru_xCr_ySe_z$ film in acid medium. The percentage of peroxide was evaluated from the following equation [14,15]:

$$\%H_2O_2 = \frac{200 i_R/N}{i_D + i_R/N} \quad (1)$$

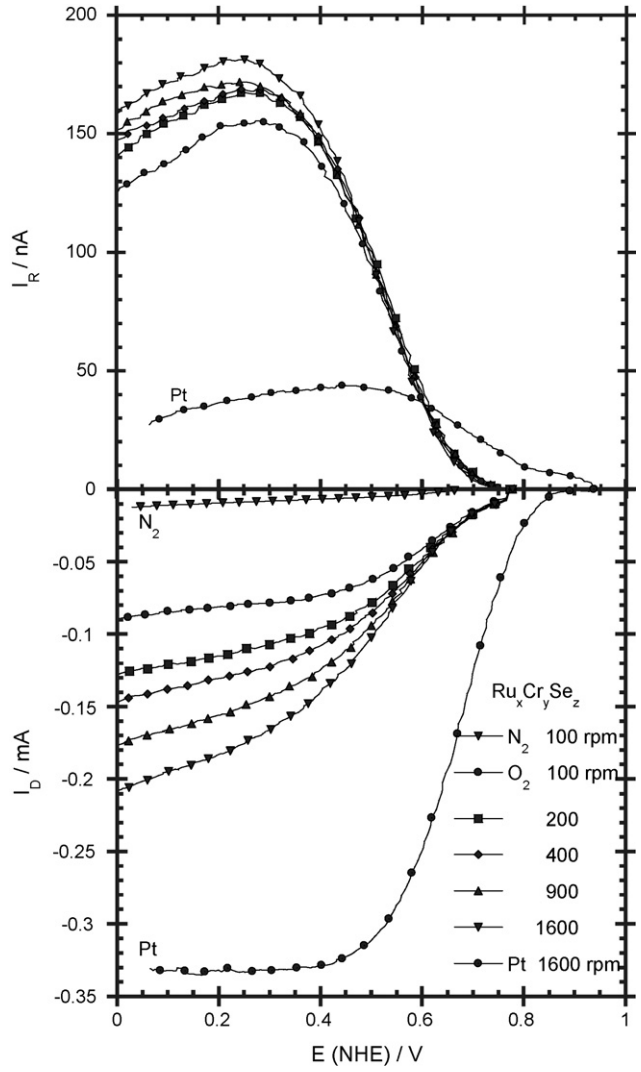

Fig. 3. Steady state polarization curves at different rotation speeds as a function of disk potentials for ORR in 0.5 M H_2SO_4. $Ru_xCr_ySe_z$ disk and Au ring held at 1.4 V/NHE. 10 wt% Pt/C disk at 1600 rpm was used for comparison.

For potentials lower than 0.65 V there is a strong voltage dependence on the hydrogen peroxide formation. The amount of H_2O_2 produced with the electrode potential in the electrochemical process of the ORR reached a maximum of 2.8% on the $Ru_xCr_ySe_z$ catalyst as determined at 0.35 V/NHE (Fig. 4), while the H_2O_2 produced on Pt disk was less than 1%. The small amount of intermediate produced in both cases suggests that the molecular oxygen was predominantly reduced to H_2O (*i.e.*, $\%H_2O = 100 - \%H_2O_2$). Kinetic analysis of the ring-disk data was carried out using the model of Damjanovic et al. [16,17] for the ORR in acidic media proposed as described bellow:

$$O_2 + 4H^+ + 4e^- \xrightarrow{k_1} 2H_2O \quad (2)$$

$$O_2 + 2H^+ + 2e^- \xrightarrow{k_2} H_2O_2 \quad (3)$$

$$H_2O_2 + 2H^+ + 2e^- \xrightarrow{k_3} 2H_2O \quad (4)$$

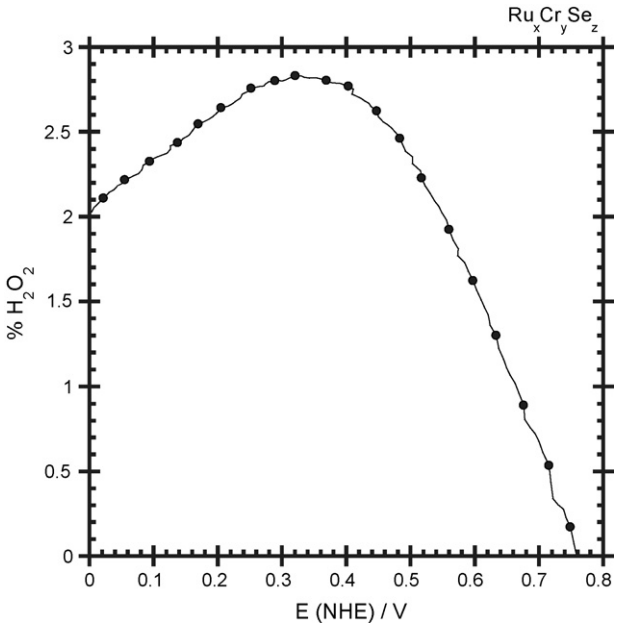

Fig. 4. Percentage of H_2O_2 produced of the molecular oxygen reduction on $Ru_xCr_ySe_z$ electrocatalyst.

The first mechanism is a direct reduction path of oxygen to water, that is, the four-electron charge transfer process. The second mechanism is a serial one in which the reduction of oxygen to hydrogen peroxide is further reduced to water.

Fig. 5 shows the rate constants evaluated over the entire potential range taking into account equations derived for k_1, k_2 and k_3 described in ref [13,18]. Since k_1 is much larger than k_2 over the explored potential range, the molecular oxygen is mainly reduced to water *via* the direct four-electron transfer path. From the kinetic results we propose to test $Ru_xCr_ySe_z$ catalyst as a cathode in a single PEMFC.

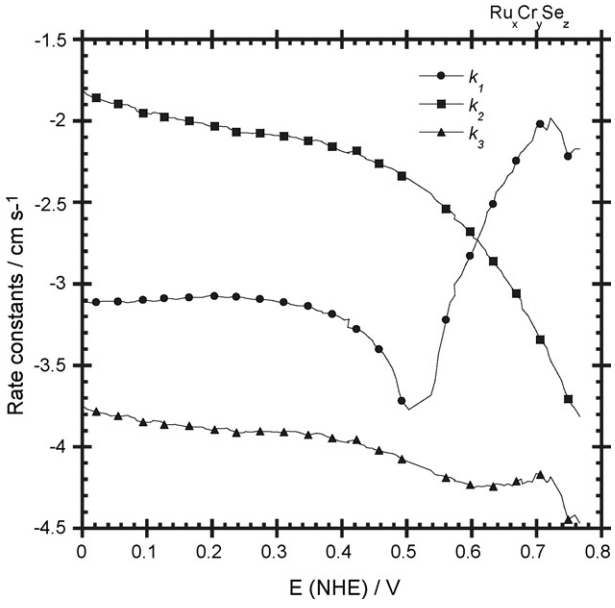

Fig. 5. Rate constants calculated for oxygen reduction reaction on $Ru_xCr_ySe_z$ catalysts based on Damjanovic's Model [16].

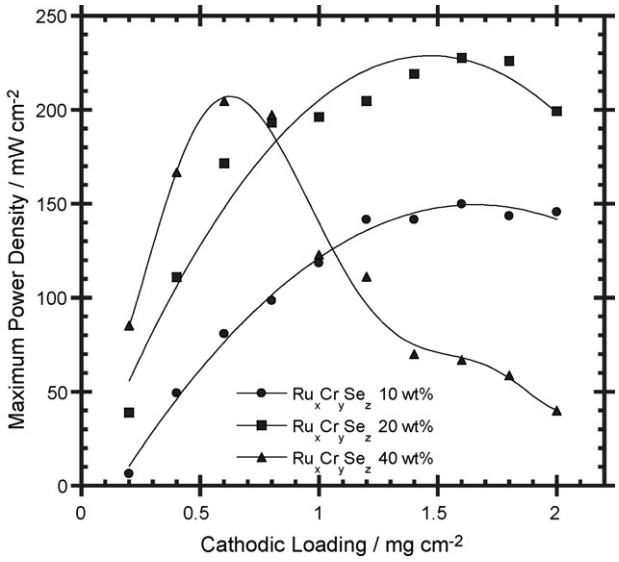

Fig. 6. Cathode catalyst loading study of $Ru_xCr_ySe_z$ catalysts versus the maximum power density obtained from each assembly.

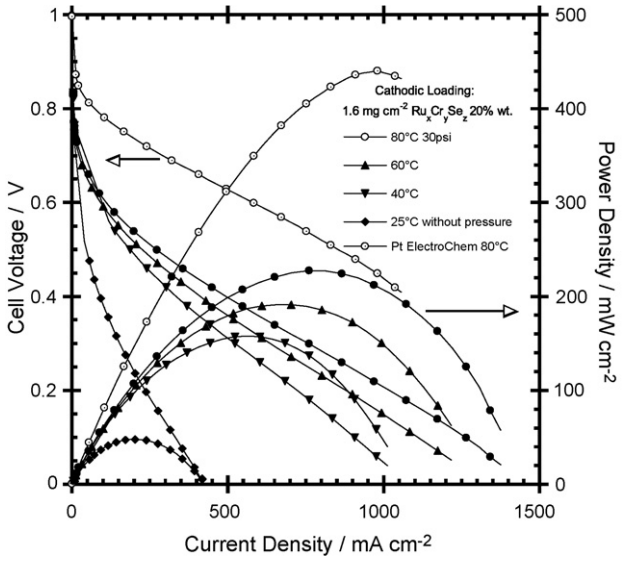

Fig. 7. Performance curves of $Ru_xCr_ySe_z$ at 20 wt%, corresponding to the best MEA response.

3.3. Membrane–electrode assembly (MEA) characterization

Fig. 6 shows the MEA performance results for the study of cathode-catalyst loading variation (mg cm^{-2}) at 10, 20 and 40 wt% of $Ru_xCr_ySe_z$ versus the maximum power density obtained in each assembly. In this figure it is observed that $Ru_xCr_ySe_z$ at 20 wt% shows the maximum performance, while $Ru_xCr_ySe_z$ 10 wt% presents an acceptable performance, whereas in $Ru_xCr_ySe_z$ 40 wt% the performance decreases with respect to the cathode catalyst loading. This behavior is attributed to the amount of catalyst per geometric area available to be reached by reactant gases and thus electrochemically active in each dispersion. This means that there should be an optimum catalyst loading where the catalyst utilization would be the best. After that, any extra particle present in the MEA could block catalyst active sites.

For any specific application, an analysis should be carried out in order to choose the best dispersion/loading arrangement (10 wt% versus 20 wt% catalyst). Fig. 7 presents the performance of 1.6 mg cm^{-2} and 20 wt% $Ru_xCr_ySe_z$ MEA, which up to now was the best assembly obtained during the catalyst loading study. The maximum in power density was about 220 mW cm^{-2} and it was reached at 0.3 V. As expected, the performance of the assembly increases as the temperature and pressure of operation increase. As observed during experimentation with this particular catalyst, the gas pressure has a greater effect on the cell performance than the cell temperature. Fig. 7 also compares the performance of the $Ru_xCr_ySe_z$ cathode catalyst with respect to a commercial ElectroChem membrane using Pt at 1 mg cm^{-2} (20 wt% Pt/C). Under the same operational and experimental conditions the $Ru_xCr_ySe_z$ performance is about 50% lower than that obtained with platinum. This output performance is attributed basically to the intrinsic properties of the cathodic reaction of the ruthenium-based catalyst on the polymeric membrane. However, there are still other options available to test with other transition metals in order to enhance the performance of the ruthenium-based catalyst or to use significantly more catalyst than the amount required for the initial kinetic activity study.

The stability curve of the MEA with 1.6 mg cm^{-2} $Ru_xCr_ySe_z$ 20 wt% as cathode is presented in Fig. 8. The MEA was kept at 0.4 V of cell voltage, 80 °C and 10 psi for 100 h of continuous operation. Operation pressure of 10 psi was chosen because of security reasons. The reached performance was roughly in average of 70 mW cm^{-2}. There were small variations in the achieved performance. Fig. 8 shows a decrease in activity from 0 to 70 h of operation. After this time the cell was purged and the activity was recuperated. A possible explanation of this behavior is the cell flooding. Cathode flooding caused by excessive liquid water has been recognized as the main reason of poor PEMFC

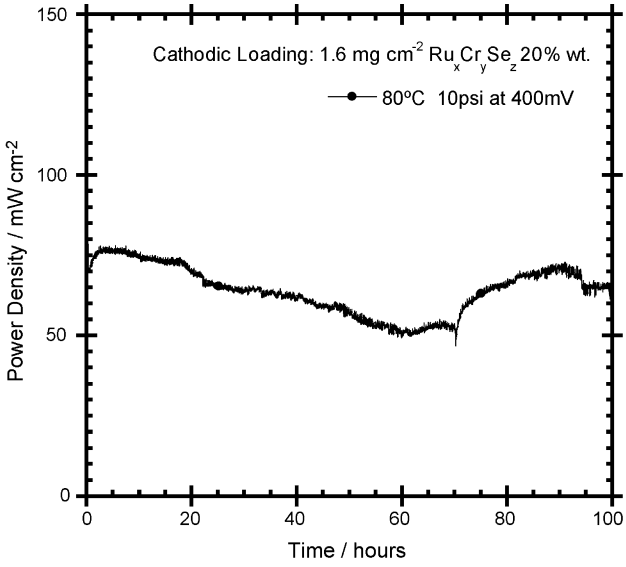

Fig. 8. Stability curve of a MEA with $Ru_xCr_ySe_z$ catalyst as cathode polarized at 0.4 V of cell voltage.

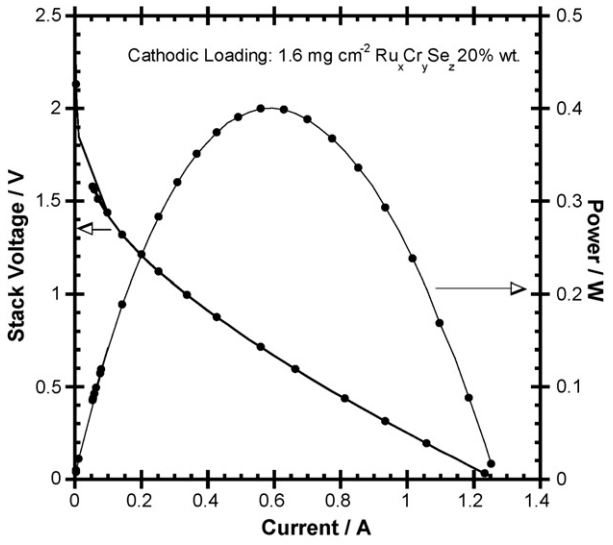

Fig. 9. PEFC stack performance at 80 °C and 10 psi.

performance [19]. This situation can be eliminated by an appropriate flow field design. This experimental result suggest that $Ru_xCr_ySe_z$ catalyst is stable for at least 100 h of continuous operation and this can be interpreted as a first indication for this material to be a suitable candidate as a cathode in H_2/O_2 – air PEMFC.

3.4. Stack characterization

Physically, the stack is a 7 cm-side cube. As described above all components were designed and manufactured in our own facilities. Fig. 9 shows the stack performance at 80 °C and 10 psi. The working pressure of 10psi was the maximum level that bipolar plates could withstand without leaks and crossover. The open circuit potential was near 2.3 V. The observed activation overpotential is related to the intrinsic properties of ruthenium-based catalysts such as electronic and geometric configuration, which is quite different to Pt-based alloys. The maximum power reached by the stack was 0.4 W. This value is somewhat low compared with those obtained in the loading optimization study. However, a design and choice of materials optimization could improve the obtained values. In order to expand the size of tested MEAs, the preparation methodology should also be improved. An optimal operation condition study is in progress using an approach based on fuel cell simulations [20–22].

4. Conclusions

The synthesized $Ru_xCr_ySe_z$ material in organic solvent has demonstrated catalytic activity for oxygen reduction in acid medium. The electrocatalyst morphology consisted of a highly rough fractal-type nanometric material with an average of 80–160 nm in size. The estimated composition of the catalyst was of $Ru_6Cr_4Se_5$ deduced from EDS analysis. Chemical and physical analysis has shown that this material presents chemical stability above the temperature range of the PEMFC operation.

The oxygen reduction reaction on $Ru_xCr_ySe_z$ proceeds mostly via the four-electron transfer process to water formation with a maximum of 2.8% of hydrogen peroxide as by-product.

MEA best performance was reached with a cathode catalyst loading of 1.6 mg cm^{-2} of 20 wt% $Ru_xCr_ySe_z$/CarbonVulcan XC-72 and anodic loading of 0.8 mg cm^{-2} of 10 wt% Pt/C (E-ETEK). Catalyst at 10 wt% presented a reasonable performance whereas catalyst at 40 wt% performance was not acceptable. For any specific application, an economic-performance analysis should be carried out in order to choose the best catalyst loading between 10 and 20 wt%. Under the same of temperature and pressure conditions the $Ru_xCr_ySe_z$ performance is near a half of the value reported for Pt. $Ru_xCr_ySe_z$ catalyst was stable for at least 100 h of continuous operation and its electrochemical behavior suggests that it could be a suitable candidate to be used as cathode in H_2/O_2 – air PEMFC. The stack performance obtained is a step in the optimum design and manufacturing know-how.

Acknowledgements

This work was partially supported by a Grant of National Science and Technology Council of Mexico, CONACYT (ref. 46094). The author (KSA) would like to thank CONACYT for providing her the doctoral fellowship. The authors thank to JG Cabañas-Moreno for his assistance in the EDS analysis and to C. Flores-Morales for the AFM images and instruction.

References

[1] H.A. Gasteiger, S.S. Kocha, B. Sompalli, F.T. Wagner, Appl. Catal. B 56 (2005) 9–35.
[2] J.H. Liu, M.K. Jeon, S.I. Woo, Appl. Surf. Sci. 252 (2006) 2580–2587.
[3] H. Boennemann, K.S. Nagabhushana, J. New Mat. Electrochem. Syst. 7 (2004) 93–108.
[4] E.S. Smotkin, R. Diaz-Morales, Ann. Rev. Mater. Res. 33 (2003) 557–579.
[5] R.G. González-Huerta, J.A. Chávez-Carvayar, O. Solorza-Feria, J. Power Sources 153 (2006) 11–17.
[6] R.G. González-Huerta, R. González-Cruz, O. Solorza-Feria, J. New. Mater. Electrochem. Syst. 8 (2005) 15–23.
[7] R. González-Cruz, O. Solorza-Feria, J. Solid State Electrochem. 7 (2003) 289–295.
[8] K. Suárez-Alcántara, A. Rodríguez-Castellanos, R. Dante, O. Solorza-Feria, J. Power Sources 157 (2006) 114–120.
[9] H. Schulenburg, M. Hilgendorff, I. Dorbandt, J. Radnik, P. Bogdanoff, S. Fiechter, M. Bron, H. Tributsch, J. Power Sources 155 (2006) 47–51.
[10] H. Cheng, W. Yuan, K. Scott, Electrochimica. Acta 52 (2006) 466–473.
[11] D. Cao, A. Wieckowski, J. Inukai, N. Alonso-Vante, J. Electrochem. Soc. 153 (2006) A869–A874.
[12] V.I. Zaikovskii, K.S. Nagabhushana, V.V. Kriventsov, K.N. Loponov, Ch. Suetlana, R.I. Kvon, H. Boennemann, D.I. Kochubey, E.R. Savinova, J. Phys. Chem. B 110 (2006) 6881–6890.
[13] S. Durón, R. Rivera, P. Nkeng, G. Poillerat, O. Solorza-Feria, J. Electroanal. Chem. 566 (2004) 281–289.
[14] H.A. Gasteiger, W. Gu, R. Makharia, M.F. Mathias, B. Sompalli, in: W. Vielstich, H.A. Gasteiger, A. Lamm (Eds.), Handbook of Fuel Cell, vol. 3, John Wiley & Sons, 2003, Chapter 46.
[15] U.A. Paulus, T.J. Schmidt, H.A. Gasteiger, R.J. Behm, J. Electroanal. Chem. 495 (2001) 134–145.
[16] A. Damjanovic, M.A. Genshaw, J.O.'M. Bockris, J. Chem. Phys. 45 (1966) 4057–4059.

[17] N.A. Anastasijevic, V. Vesovic, R.R. Adzic, J. Electroanal. Chem. 229 (1987) 305–316.
[18] S. Durón, R. Rivera, G. Poillerat, O. Solorza-Feria, J. New Mat. Electrochem. Syst. 4 (2001) 17–23.
[19] T.V. Nguyen, W. He, in: W. Vielstich, H.A. Gasteiger, A. Lamm (Eds.), Handbook of Fuel Cell, vol. 3, John Wiley & Sons, 2003, Chapter 28.
[20] R.C. Dante, J.L. Escamilla, V. Madrigal, T. Theus, J. Calderon, O. Solorza, R. Rivera, Int. J. Hydrogen Energy 28 (2003) 343–348.
[21] R.C. Dante, J. Lehmann, O. Solorza-Feria, J. Appl. Electrochem. 35 (2005) 327–337.
[22] R.C. Dante, F. Menzl, J. Lehmann, C. Sponholz, O. Luschtinetz, O. Solorza-Feria, J. Appl. Electrochem. 36 (2006) 187–193.